ACS OMEGA

http://pubs.acs.org/journal/acsodf

Article

Designing BH3-Mimetic Peptide Inhibitors for the Viral Bcl-2 Homologues A179L and BHRF1: Importance of Long-Range Electrostatic Interactions

Chinthakunta Narendra Reddy and Ramasubbu Sankararamakrishnan*

Cite This: *ACS Omega* 2021, 6, 26976−26989

Read Online

ACCESS | Metrics & More | Article Recommendations | Supporting Information

ABSTRACT: Viruses have evolved strategies to prevent apoptosis of infected cells at early stages of infection. The viral proteins (vBcl-2s) from specific viral genes adopt a helical fold that is structurally similar to that of mammalian antiapoptotic Bcl-2 proteins and exhibit little sequence similarity. Hence, vBcl-2 homologues are attractive targets to prevent viral infection. However, very few studies have focused on developing inhibitors for vBcl-2 homologues. In this study, we have considered two vBcl-2 homologues, A179L from African swine fever virus and BHRF1 from Epstein−Barr virus. We generated two sets of 8000 randomized BH3-like sequences from eight wild-type proapoptotic BH3 peptides. During this process, the four conserved hydrophobic residues and an Asp residue were retained at their respective positions, and all other positions were substituted randomly without any bias. We constructed 8000 structures each for A179L and BHRF1 in complex with BH3-like sequences. Histograms of interaction energies calculated between the peptide and the protein resulted in negatively skewed distributions. The BH3-like peptides with high helical propensities selected from the negative tail of the respective interaction energy distributions exhibited more favorable interactions with A179L and BHRF1, and they are rich in basic residues. Molecular dynamics studies and electrostatic potential maps further revealed that both acidic and basic residues favorably interact with A179L, while only basic residues have the most favorable interactions with BHRF1. As in mammalian homologues, the role of long-range interactions and nonhotspot residues has to be taken into account while designing specific BH3-mimetic inhibitors for vBcl-2 homologues.

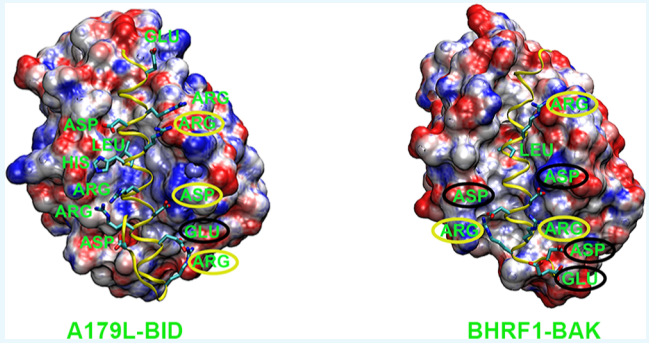

INTRODUCTION

The immediate response of viral infection in mammals includes programmed cell death (PCD) of infected cells and immune response. Among the many different types of cell deaths, apoptosis is an important mode of PCD in mammalian cells and can occur either via extrinsic or intrinsic pathways.[1] The intrinsic pathway or mitochondrial apoptosis is mediated by the Bcl-2 family of proteins, and the family members include those that promote (proapoptotic) or oppose (antiapoptotic) cell death.[2,3] Antiapoptotic Bcl-2 members are characterized by the presence of multi Bcl-2 homology (BH) domains (BH1 to BH4), while proapoptotic members have either multi BH domains (BH1 to BH3) or only the BH3 domain.[4,5] "BH3-only" proapoptotic proteins can be activators of proapoptotic Bak/Bax or can be repressors antagonizing the antiapoptotic Bcl-2 proteins such as Bcl-X_L or Mcl-1.[6,7] Upon activation, Bax/Bak accumulate on the mitochondrial surface and form pores in mitochondrial outer membranes. This process enables apoptogenic proteins such as cytochrome *C* to be released in the cytoplasm, leading to eventual cell death.[8,9] At the initial stages of infection, viruses have evolved mechanisms to inhibit apoptosis to avoid early cell death that will help the virus to replicate.[10−12] This is achieved through viral proteins that mimic the mammalian antiapoptotic Bcl-2 proteins. Many viral Bcl-2 homologues (vBcl-2) are structurally similar to their mammalian counterparts with distinct Bcl-2 α-helical fold.[13−16] However, they exhibit little or no sequence similarity to the antiapoptotic Bcl-2 proteins. Examples include F1L and N1 from vaccinia virus (PDB ID: 2VTY and 2UXE),[17,18] M11L from myxoma virus (PDB ID: 2O42),[19] BHRF1 from Epstein−Barr virus (EBV) (PDB ID: 2WH6),[20] KsBcl-2 from Kaposi sarcoma herpesvirus (PDB ID: 1K3K),[21] F1L from Variola virus (PDB ID: 5AJJ),[22] M11 from γ-herpesvirus 68 (PDB ID: 2ABO),[23] ORFV125 from ORF virus (PDB ID: 7ADS),[24] GIV66 from grouper iridovirus

Received: June 28, 2021
Accepted: September 16, 2021
Published: October 4, 2021

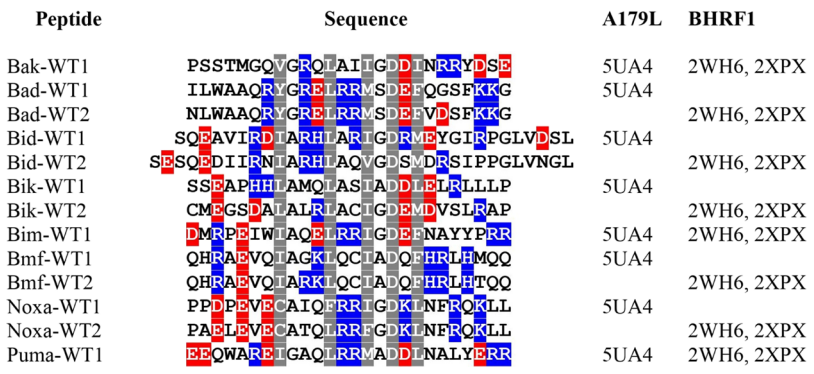

Figure 1. Sequences of wild-type BH3 peptides from proapoptotic proteins that are used to derive BH3-like sequences. The residues which are retained while deriving BH3-like sequences are shown in a gray background. Residues shown in red and blue backgrounds represent acidic and basic residues, respectively. PDB IDs of template structures which are used to model A179L and BHRF1 complex structures are provided.

(PDB ID: 5VMN),[25] CNP058 from canarypox virus (PDB ID: 5WOS),[26] FPV039 from fowlpox virus (PDB ID: 5TZP),[27] 16L protein from tanapoxvirus (PDB ID: 6TQP),[28] and A179L from African swine fever virus (PDB ID: 5UA4).[29] These viruses cause diseases such as canarypox (song birds), smallpox (humans), myxomatosis (rabbits), Burkitt's lymphoma, Hodgkin and non-Hodgkin lymphoma and other cancers (humans), Castleman's disease (humans), contagious ecthyma (sheep and goats), sleepy grouper disease (fish), fowlpox (chicken), and African swine fever (pigs and warthogs).[30−37] Thus, the viral diseases can be lethal to humans and/or economically devastating. Hence, understanding the molecular mechanism of viral infection at the early stages of viral entry into host cells is an important step in curtailing the viral diseases.

In mammalian antiapoptotic Bcl-2 proteins, it has been shown that the peptide corresponding to the BH3 domain of proapoptotic counterparts is enough to trigger the apoptotic process.[38,39] Several antiapoptotic Bcl-2 proteins exhibit different affinities for proapoptotic BH3 peptides.[40,41] While Bim binds to all antiapoptotic Bcl-2 proteins, Bad binds to only Bcl-X_L, Bcl-2 and Bcl-w and does not bind to Mcl-1 and A1. Similarly, Noxa binds to Mcl-1 and A1 but has no affinity for Bcl-X_L, Bcl-w, and Bcl-2. Binding studies for viral Bcl-2 homologues reveal that each vBcl-2 homologue has its own binding profile, and many times, they differ from mammalian prosurvival proteins.[14,17,20,22,27,29,42−45] Binding profiles of the vBcl-2 homologue from African swine fever virus A179L show that it is a pan-proapoptotic Bcl-2 binder, binding to all BH3 motifs of various prodeath Bcl-2 proteins tested.[29] On the other hand, F1L from vaccinia virus binds only to a limited number of proapoptotic BH3 peptides.[17]

Structural studies have shown that the proapoptotic BH3 peptides bind to the hydrophobic groove formed by many amphipathic α-helices of prosurvival Bcl-2 proteins.[15,16,38] Efforts to design small molecules that mimic the proapoptotic BH3 domain have been successful to some extent, and some of them have reached clinical trials.[46,47] However, these molecules are designed to antagonize mammalian antiapoptotic Bcl-2 proteins. As vBcl-2s adopt a similar structural fold, one can imagine that the inhibitors developed for antiapoptotic Bcl-2 proteins can also act on vBcl-2s. Robert et al. tested ABT-737, a small molecule that specifically inhibits Bcl-2, Bcl-X_L, and Bcl-w, on EBV-induced lymphoproliferative disorders such as Burkitt's lymphoma.[48] This drug, alone or in combination with other conventional drugs, did not show any improvement on the overall survival of Burkitt's lymphoma xenograft mice. Burrer et al. identified the BH3-mimetic peptide that can selectively bind vBcl-2 from Kaposi's sarcoma-associated herpesvirus by screening BH3 peptide libraries.[49] However, the identified peptide could not cross the plasma membrane. There are few reports available describing the design of specific inhibitors for inactivating viral Bcl-2 homologues.[50] Recently, Baker and his colleagues designed a novel protein that can bind to BHRF1 of EBV with high affinity, and their structural studies showed that this protein binds to the hydrophobic groove of BHRF1 and makes many additional contacts outside this region also.[51] They also demonstrated that this protein triggers apoptosis in EBV-infected cell lines. In the mouse xenograft disease model, the designed protein could suppress tumor progression and extended the lifespan of infected mice. Although these studies show promise in developing inhibitors specific to vBcl-2, these are too few compared to the numerous studies reported in the literature describing the design and development of inhibitors for mammalian antiapoptotic Bcl-2 proteins. Hence, it is important that specific focus should be given in developing vBcl-2-specific inhibitors that can be used in immunocompromised infected patients.

We have recently developed a computational method to design BH3-like peptides that can bind specifically to either Bcl-X_L or Mcl-1.[52] Our studies showed that BH3-mimetic peptides have distinct preference for charged residues when they bind to Mcl-1 or Bcl-X_L and also highlighted the role of long-range electrostatic interactions due to nonhotspot residues. The computationally designed BH3 peptide inhibitors, predicted to bind Mcl-1 or Bcl-X_L with high affinity, were successfully validated in cell viability and cell proliferation studies. In the current study, we have applied the same approach to design BH3-like peptides for two of the vBcl-2 homologues, BHRF1 from EBV and A179L from African swine fever virus. A179L binds to all proapoptotic BH3 peptides,[29] while BHRF binds to a subset of them with high affinity including Bak and Bim.[20] Results of this study show that the designed BH3-mimetic peptides are rich in basic residues for both BHRF1 and A179L. However, the pattern of interactions between the charged residues and the protein seems to differ between BHRF1 and A179L.

RESULTS

Wild-type BH3 sequences from proapoptotic Bcl-2 proteins were used to generate randomized BH3-like sequences (Figure

https://doi.org/10.1021/acsomega.1c03385
ACS Omega 2021, 6, 26976−26989

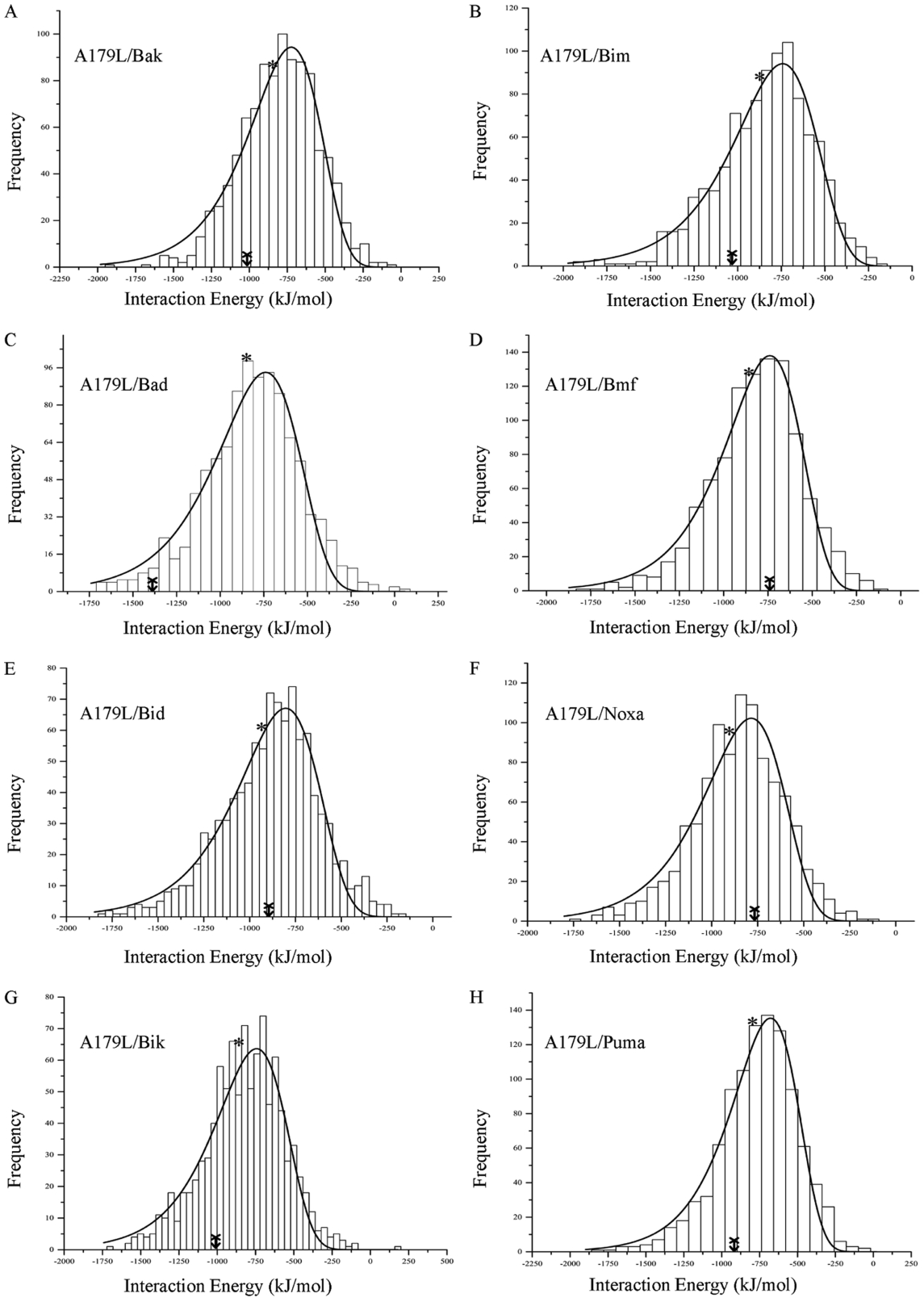

Figure 2. Histograms of interaction energies between A179L and BH3-like sequences. The wild-type BH3 peptides from which the BH3-like sequences were derived are indicated in each histogram: (A) Bak, (B) Bim, (C) Bad, (D) Bmf, (E) Bid, (F) Noxa, (G) Bik, and (H) Puma. In each histogram, the mean value and the interaction energy of the wild-type BH3 peptide are designated with an asterisk and arrow, respectively.

1), as described in the Materials and Methods section. We considered a total of eight BH3 wild-type sequences from Bak, Bad, Bid, Bik, Bim, Bmf, Noxa, and Puma, and in each case, we generated two sets of 1000 BH3-like sequences. Structures of BH3-like sequences in complex with A179L were modeled as described in the Materials and Methods section. The same exercise was repeated for generating BHRF1/BH3-like peptide complex structures. In total, we modeled 16,000 complex

https://doi.org/10.1021/acsomega.1c03385
ACS Omega 2021, 6, 26976−26989

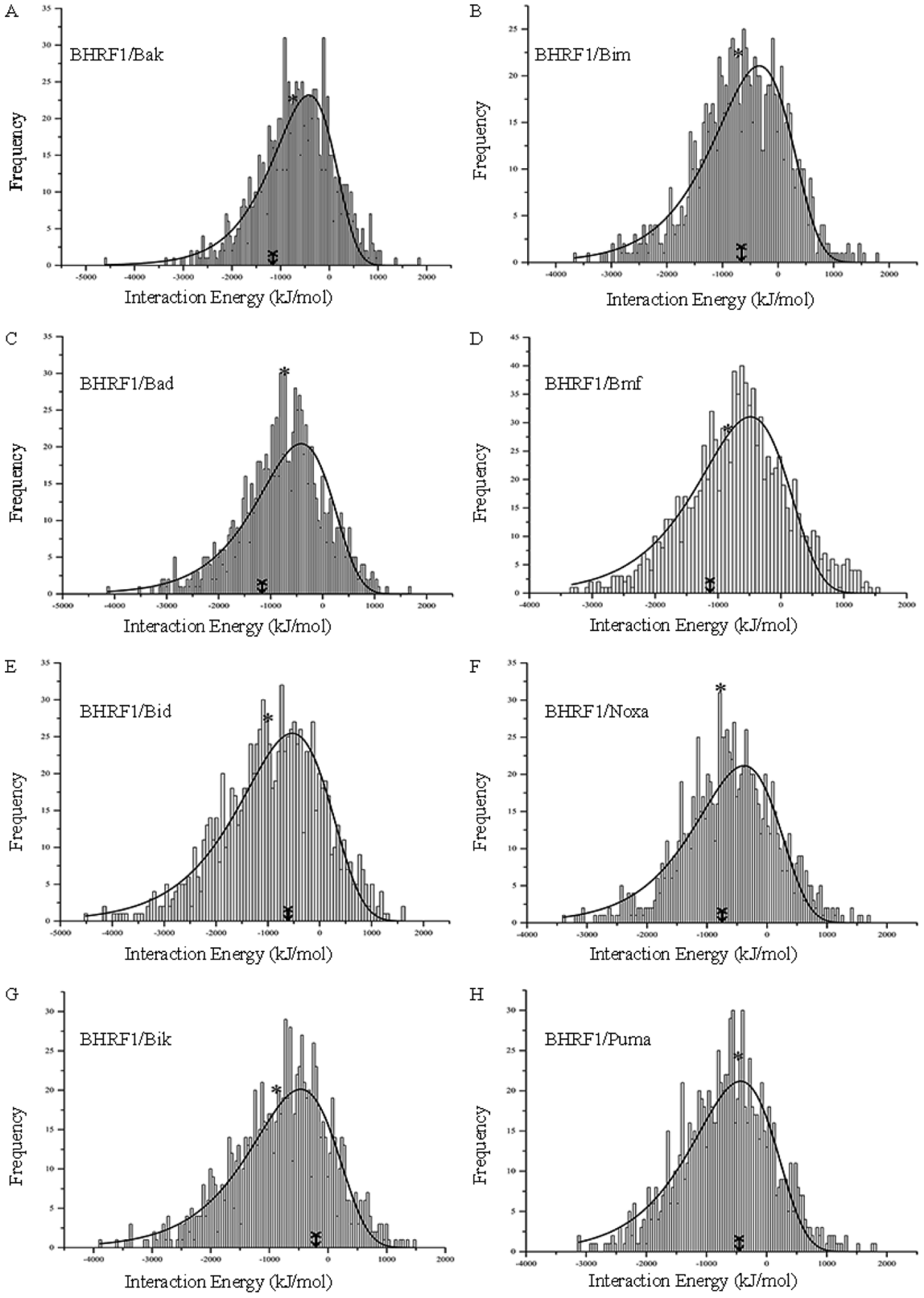

Figure 3. Histograms of interaction energies between BHRF1 and BH3-like sequences. The wild-type BH3 peptides from which the BH3-like sequences were derived are labeled in each histogram: (A) Bak, (B) Bim, (C) Bad, (D) Bmf, (E) Bid, (F) Noxa, (G) Bik, and (H) Puma. The mean value and the interaction energy of the wild-type BH3 peptide in each histogram are designated with an asterisk and arrow, respectively.

structures (8000 each for A179L and BHRF1 systems). Interaction energies between the peptide and protein (A179L or BHRF1) were calculated (see the Materials and Methods section). Histograms of interaction energies of peptide/protein for BH3-like sequences derived from each wild-type BH3 peptide were plotted and are shown in Figures 2 and 3 for A179L and BHRF1, respectively. It is evident that the interaction energies show negatively skewed extreme value

https://doi.org/10.1021/acsomega.1c03385
ACS Omega 2021, 6, 26976−26989

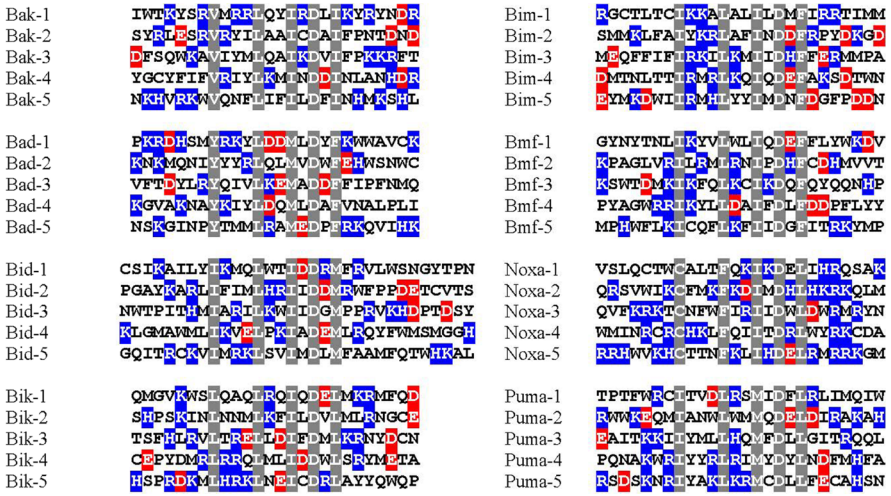

Figure 4. Top BH3-like sequences with high helical propensities and the most favorable interaction energies with A179L selected from the extreme negative tail regions of the respective interaction energy histograms (see Figure 2). The acidic, basic, and conserved residues are shown in red, blue, and gray backgrounds, respectively.

distributions. We made a similar observation for mammalian antiapoptotic Bcl-2 proteins also.[52] In majority of the cases, the interaction energy of the wild-type peptide lies close to or within one standard deviation from the mean value. The BH3-like sequences whose interaction energies lie in the extreme negative tail region have the most favorable interactions with the protein. Hence, our interest is to select BH3-like sequences from this region which are predicted to have higher helicity and a mean helical hydrophobic moment. It has been shown that helical stability of BH3 peptides is directly correlated with the binding affinity and the BH3 domain forms amphipathic helices in naturally occurring proapoptotic proteins.[53−55] For each wild-type BH3 peptide, we selected five BH3-like sequences from the extreme negative tail region of histograms with high predicted helicity. Helicity and the mean helical hydrophobic moment of each BH3-peptide were predicted using Agadir and HeliQuest web servers.[56−59] We analyzed interaction energies of these selected peptides with the protein. The van der Waals and Coulombic components of interaction energies calculated for BH3-like sequences are compared with the corresponding wild-type proapoptotic BH3 peptide from which these sequences were derived. The following sections will first discuss the findings independently for A179L and BHRF1, and then, the results for these proteins will be compared between them and also with respect to the mammalian antiapoptotic proteins Bcl-X_L and Mcl-1.

A179L in Complex with BH3-like Sequences. We have selected top five BH3-like peptides derived from each of the eight wild-type proapoptotic BH3 sequences. These top BH3-like peptides were selected from the negative tail region of interaction energy distributions obtained for A179L modeled complex structures (Figure 2). The sequences of these peptides are shown in Figure 4, and their predicted helical propensities (Figure S1A) are significantly higher than that of the corresponding wild-type BH3 peptides. The mean helical hydrophobic moment calculated for each BH3-like sequence is comparable to that of the wild-type BH3 sequence from which they are derived (Figure S2A). The five selected BH3-like sequences derived from Bak are designated as Bak-1 to Bak-5. A similar notation was used for BH3-like sequences derived from other proapoptotic wild-type BH3 peptides. The selected sequences clearly show a pattern, and they are rich in basic residues. The net charge of the majority of these peptides varies from +1 to +9. Interaction energies of each of the selected BH3-like peptide in complex with A179L are plotted in Figure 5A. It is very clear that the BH3-like sequences interact with A179L much more favorably than the corresponding wild-type BH3 peptides. Interaction energies calculated for the wild-type peptides vary from −740 kJ/mol (Bmf-WT) to −1388 kJ/mol (Bad-WT). The BH3-like sequences derived from the wild-type BH3 peptides interact with A179L with interaction energies ranging from −1321 to −1814 kJ/mol. In all the cases, the BH3-like sequences interact with A179L more favorably by 300 to 900 kJ/mol. Only Bad-3 interacts with A179L with similar interaction energy to that of wild-type Bad. When we examined the histogram of interaction energies of BH3-like sequences derived from Bad, we observe that the Bad wild-type peptide's interaction energy with A179L lies near the negative tail of the distribution, indicating that the Bad wild-type sequence is already optimized to interact with A179L with the most favorable interaction energy. The Coulombic component of interaction energies (Figure 5B) significantly contributes to the total interaction energies, while van der Waals interaction energies between the selected peptides and A179L are comparable to the wild type (Figure S3A). This indicates that the electrostatic interactions due to charged residues in the peptides play a major role in giving rise to highly favorable interaction energies with A179L.

BHRF1/BH3-like Peptide Complex Structures. The top five selected BH3-like sequences derived from each of the eight wild-type proapoptotic BH3 peptides are shown in Figure 6. These peptides were from the extreme negative tail of regions of interaction energy distributions for BHRF1 complex structures (Figure 3). A majority of the selected peptides have helical propensities significantly higher than that of wild-type BH3 peptides (Figure S1B). In most of the cases, the calculated mean helical hydrophobic moments are comparable to the corresponding wild-type BH3 peptides (Figure S2B). The five selected BH3-like peptides that are derived from the wild-type Bak BH3 peptide are labeled Bak-a to Bak-e. The same notation is followed for other BH3-like peptides also, and this will help distinguish from the BH3-like peptides that are

https://doi.org/10.1021/acsomega.1c03385
ACS Omega 2021, 6, 26976−26989

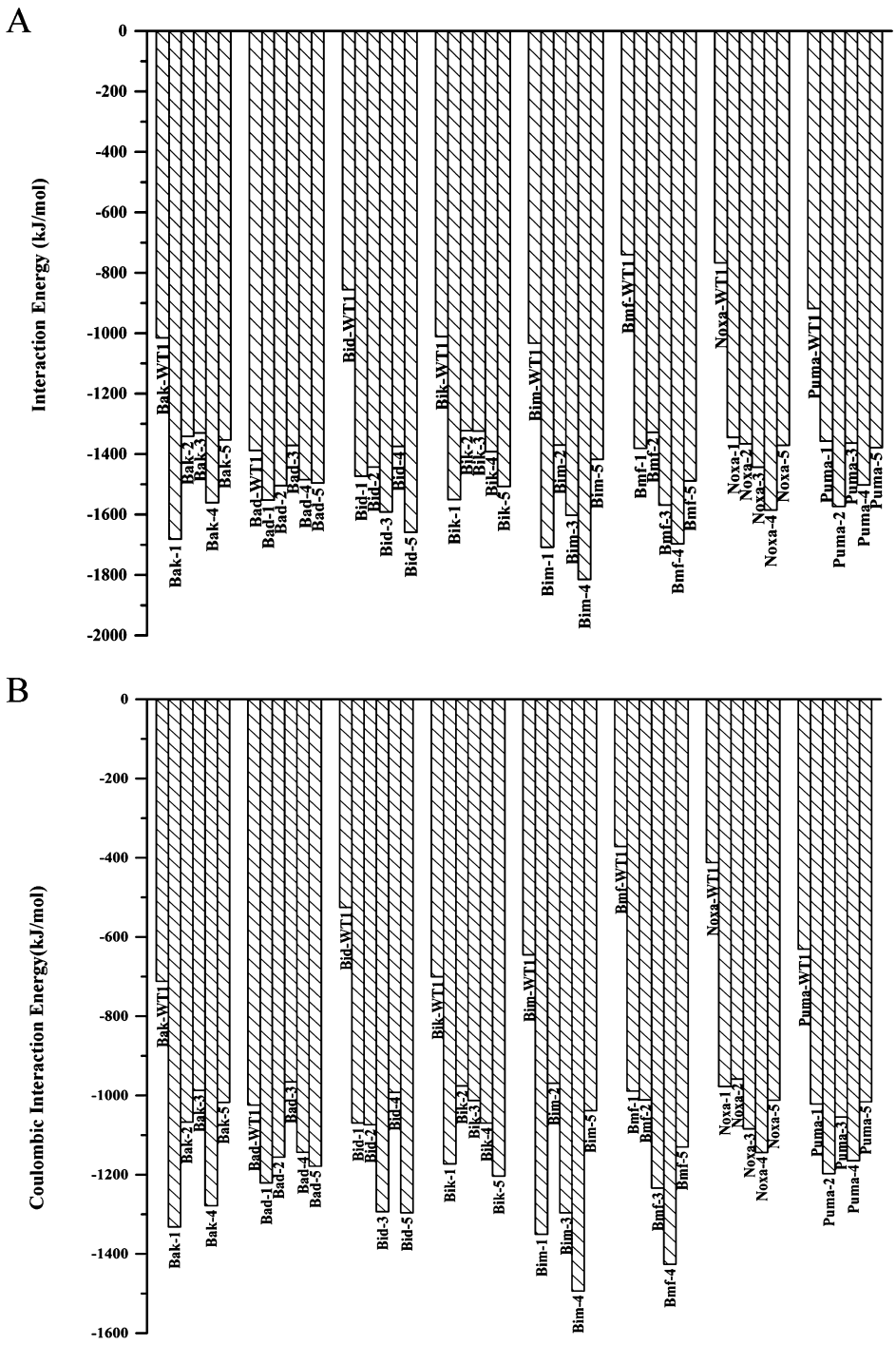

Figure 5. (A) Interaction energies of wild-type BH3 peptides and top selected BH3-like peptides in complex with A179L. (B) Electrostatic components of interaction energies of BH3 wild-type peptides and BH3-like sequences when bound to A179L.

used to model A179L complex structures. When we examined the BH3-like sequences derived from various wild-type proapoptotic BH3 regions, they are strikingly rich in basic residues. The net charge of the peptides varied from +1 to +7. Interaction energies of each set of BH3-like sequences derived from a specific proapoptotic BH3 domain clearly demonstrate that the wild-type proapoptotic BH3 peptides interact with BHRF1 at least 1000 kJ/mol less favorable than the BH3-like peptides (Figure 7A). When wild-type BH3 peptides interact with BHRF1, the interaction energies range from −206 (Bik-WT) to −1170 (Bak-WT) kJ/mol. However, the BH3-like sequences derived from wild-type proapoptotic BH3 domains interact with BHRF1 with interaction energies varying from −1875 to −3830 kJ/mol. The differences in interaction energies are especially pronounced for the BH3-like peptides derived from Bik and Puma wild-type BH3 peptides. It is important to note that the interaction energies of wild-type BH3 peptides lie close to the average values of their respective distributions in the histograms. For the Bik and Puma wild-type peptides, the interaction energies are more toward the positive side of the distributions. We have also calculated the Coulombic and van der Waals component of the interaction

https://doi.org/10.1021/acsomega.1c03385
ACS Omega 2021, 6, 26976−26989

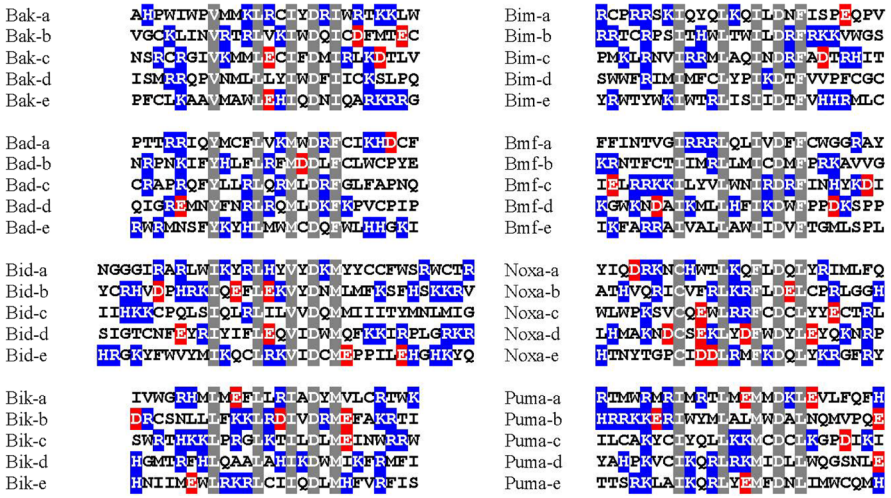

Figure 6. Top BH3-like peptides selected from the extreme negative tail end of interaction energy histograms (Figure 3). These peptides have high helical propensities and highly favorable interaction energies with BHRF1. The conserved hydrophobic residues and the conserved Asp are shown in a gray background. The acidic and basic residues are displayed in red and blue backgrounds, respectively.

energies (Figures 7B and S3B). It is evident that the major differences between the wild-type BH3 and BH3-like sequences are due to the electrostatic interactions. There is only a marginal difference in the van der Waals component. It is especially important to note that the Coulombic component of interaction energies for Bik and Puma wild-type BH3 peptides are positive.

Molecular Dynamics Simulations of Selected A179L and BHRF1 Complex Structures. Interaction energies calculated from the minimized complex structures gave an idea of the BH3-like peptides that prefer to bind to A179L or BHRF1 vBcl-2 homologues. However, it is possible that the interactions in the minimized structures may be transient and new interactions may form as protein/peptide complexes may evolve over a period of time. Hence, we carried out molecular dynamics (MD) simulations on selected complex structures and compared the results with that of wild-type BH3 peptides in complex with A179L or BHRF1. MD simulations were performed as described in the Materials and Methods section. For A179L, we selected three BH3-like peptides (Bid-5, Bim-3, and Bmf-4). Similarly, we picked four BH3-like peptides in complex with BHRF1 (Bak-c, Bik-e, Bim-c, and Noxa-c). These peptides were specifically chosen because they have high predicted helical propensity and exhibited the most favorable interaction energies compared to their respective wild-type BH3 sequences. We performed 500 ns production run for each complex structure and compared the results with the A179L/BHRF1 structure in complex with proapoptotic wild-type BH3 peptides. A total of 14 simulations were carried out for a period of 7 μs (Table S1). We have analyzed several properties including BH3 peptide helical stability and peptide/protein interaction energies.

DSSP plots of wild-type BH3 and BH3-like peptides bound to both A179L and BHRF1 show that the BH3 helical regions are mostly stable during the production runs (data not shown). The initial protein/peptide complex structure and the MD-simulated complex structure saved at the end of 500 ns production run are shown in Figure S4 and S5 for each simulated system. It is evident that both BH3 wild-type peptides and the BH3-like peptides have mostly stable helical structures. Since the BH3-like sequences selected from the extreme negative tail regions of interaction energy distributions are rich in basic residues, we calculated the average interaction energies between the charged residues of the peptide and A179L/BHRF1 protein (Figures 8 and 9) for all the simulated systems. When BH3-like peptides, Bmf-4 and Bid-5, and the wild-type BH3 peptides interact with A179L, both acidic and basic residues interact favorably with the protein (Figure 8). In the case of Bim-3, interaction energies of the acidic residues are slightly unfavorable. In general, the interaction energies of basic residues dominate, giving rise to the overall favorable interaction energies between the peptides and the protein. This also can be explained on the basis of the electrostatic potential map of A179L (Figure 10B). The protein A179L has many acidic patches explaining why many basic residues are found in most favorably interacting BH3-like sequences. However, there are also regions of basic patches that can give favorable interactions from acidic residues. By interacting with complementary regions, both acidic and basic residues result in more favorable interaction energies, and the charged residues, both positive and negative, seem to contribute to the highly favorable interaction energies as far as A179L is concerned (Figure 8).

The BH3-like sequences show a similar trend while interacting with BHRF1 and are enriched with basic residues. MD simulations of selected BH3-like sequences demonstrate that interaction energies of basic residues are the most favorable with BHRF1. The electrostatic potential map of BHRF1 reveals several acidic patches (Figure 10C), indicating that the basic residues of BH3-like sequences can interact with these regions most favorably. However, unlike A179L, the acidic residues present in BH3-like sequences interact with BHRF1 with pronounced positive interaction energies (Figure 9). This is very well compensated by the favorable interaction energies of basic residues with BHRF1 which result in the overall highly favorable Coulombic interaction energies between the BH3-like sequences and BHRF1.

We have shown electrostatic potential maps of A179L and BHRF1 along with the bound BH3 peptides as representative examples (Figure 11). When A179L interacts with the Bid wild-type BH3 peptide and Bid-5, the charged residues in both peptides result in favorable interactions (Figure 11A,B). This is

https://doi.org/10.1021/acsomega.1c03385
ACS Omega 2021, 6, 26976−26989

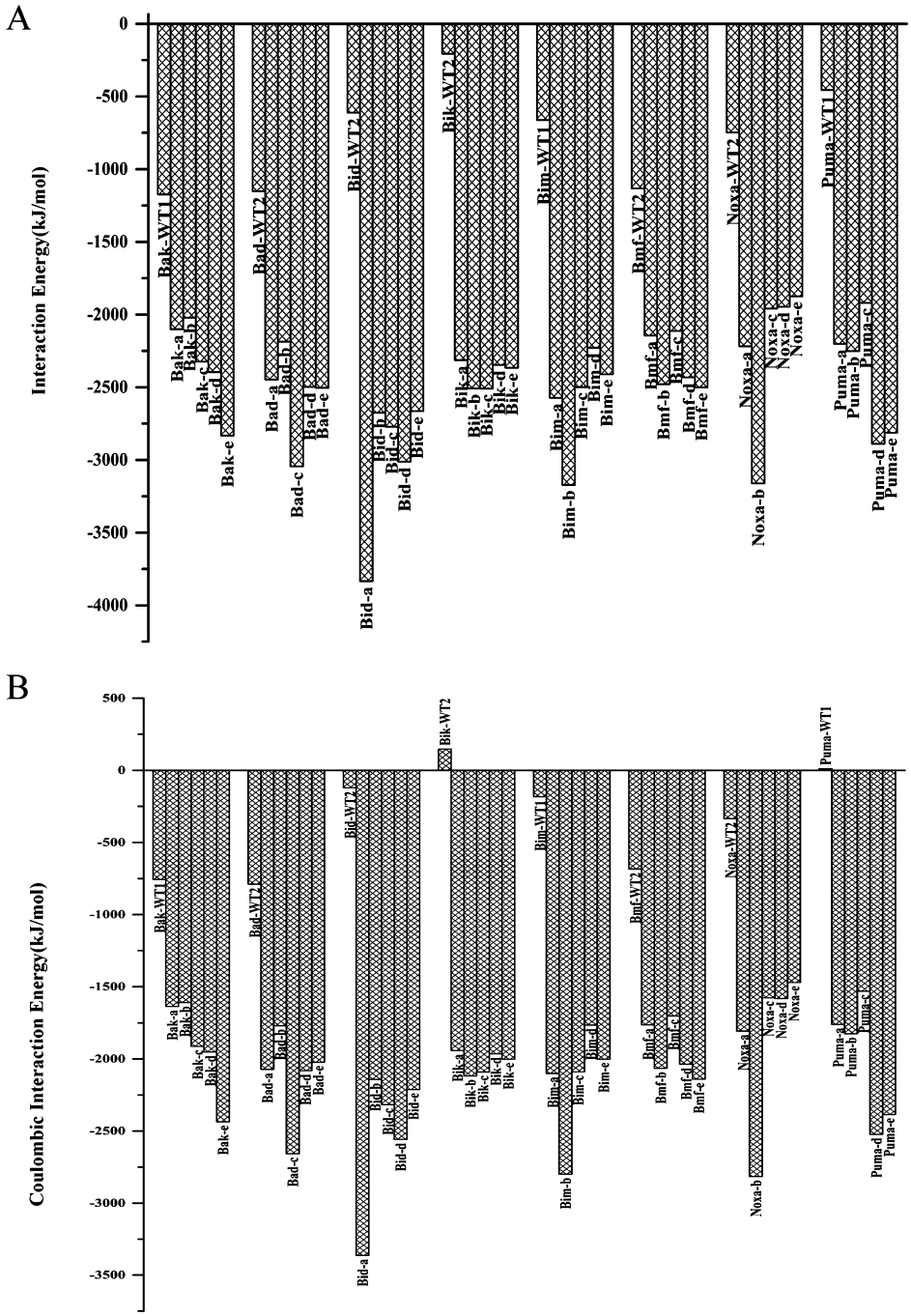

Figure 7. (A) Interaction energies of wild-type BH3 peptides and top selected BH3-like peptides in complex with BHRF1. (B) Electrostatic components of interaction energies of BH3 wild-type peptides and BH3-like sequences when bound to BHRF1.

clear from the interactions of acidic and basic residues of the peptides with the complementary regions in the protein. However, in the case of BHRF1, the acidic residues of Bak and Bak-c can be seen proximal to the negatively charged regions of BHRF1, especially toward the C-terminal segment of the peptide (Figure 11C,D). On the other hand, the basic residues of the peptides can be seen interacting with the acidic patches of the protein. To further validate this observation, we calculated the interaction energies between individual charged residues of the BH3 wild-type/BH3-like peptides and the protein for the same systems shown in Figure 11 (Table S2). This analysis clearly shows that the electrostatic interactions due to charged residues play a significant role in the protein/peptide interactions. The charged residues contribute nearly 60% of the total interaction energy in the case of A179L when it is in complex with both the wild-type Bid and the Bid-5. We can see that favorable interaction energies are contributed by both acidic and basic residues when they interact with A179L. However, it should be noted that the strength of the interactions of charged residues in Bid-5 is twice that found in Bid-WT1 (−1182 vs −590 kJ/mol). In the case of BHRF1, charged residues contribute about 28 and 61% when it is bound to Bak-WT1 and Bak-c, respectively. Interaction energies from the negatively charged Asp and Glu residues of BH3 peptides are the least favorable, especially in the case of Bak-WT1. This reduces the contribution of charged residues

https://doi.org/10.1021/acsomega.1c03385
ACS Omega 2021, 6, 26976−26989

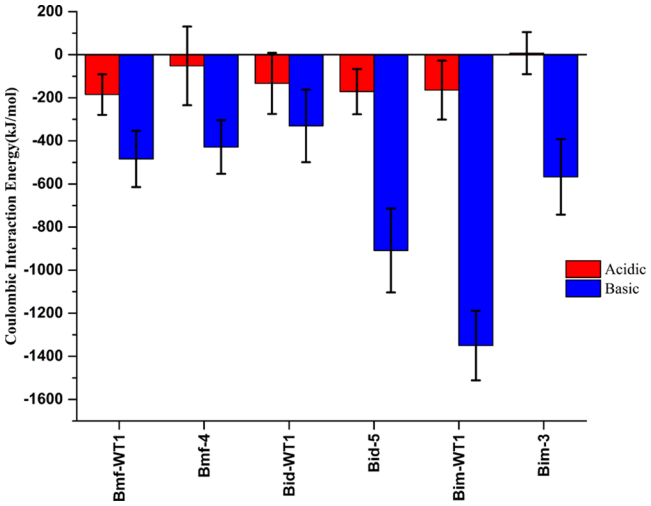

Figure 8. Average electrostatic interaction energies of A179L in complex with BH3-like sequences Bmf-4, Bid-5, and Bim-3 calculated from MD-simulated structures. For comparison purpose, average electrostatic interaction energies of A179 in complex with the respective wild-type BH3 peptides are also shown. Electrostatic interactions calculated for acidic (red) and basic (blue) residues of the BH3 or BH3-like peptides are displayed separately.

toward the total interaction energy between BHRF1 and BH3 peptides. This could be considered as one of the major differences between A179L and BHRF1. The other major distinguishing feature is the differences in the peptide/protein interaction energies between the wild-type BH3 peptides and the BH3-like sequences derived from them. In the case of BHRF1, this difference is significantly larger than that found for A179L.

DISCUSSION

The computational approach used in this study helped design BH3-mimetic peptides that can bind and interact favorably with two viral Bcl-2 homologues A179L and BHRF1. These BH3-mimetic peptides are rich in basic residues and are involved in highly favorable long-range electrostatic interactions with the respective proteins. In a previous study, we carried out similar investigation on two mammalian anti-apoptotic Bcl-2 proteins, Mcl-1 and Bcl-X_L.[52] A comparison of BH3-mimetic peptide sequences that bind to vBcl-2s and mammalian antiapoptotic Bcl-2 proteins will help us understand the major differences between these homologues, and this knowledge is likely to provide an explanation why the inhibitors developed for mammalian prosurvival Bcl-2 proteins do not have the same effect in vBcl-2 homologues.

BH3-like sequences interacting favorably with Mcl-1 and Bcl-X_L showed distinct and specific preference for charged residues. BH3-like peptides enriched with acidic residues exhibited highly favorable interactions with Mcl-1, while the peptides with predominantly basic residues interacted favorably with Bcl-X_L. Cell viability and cell proliferation studies on selected BH3-like peptides confirmed our prediction that these peptides indeed bind selectively to Mcl-1 or Bcl-X_L.[52] Since the entropic component of ligand binding to hydrophobic grooves of the proteins is unfavorable,[62] the free energy of binding of BH3 peptides to antiapoptotic proteins is largely dependent on enthalpic contribution. Thus, the interaction energy between the peptide and the protein is an indicator of binding strength and affinity. Previous studies by Bond and co-workers also considered only the enthalpic component while studying the specificities and affinities of Bcl-2 family members.[63] Hence, we extended our earlier approach to two vBcl-2 homologues, A179L and BHRF1. Both the vBcl-2 homologues considered in this study displayed preferences for BH3-like sequences with basic residues. Comparison of

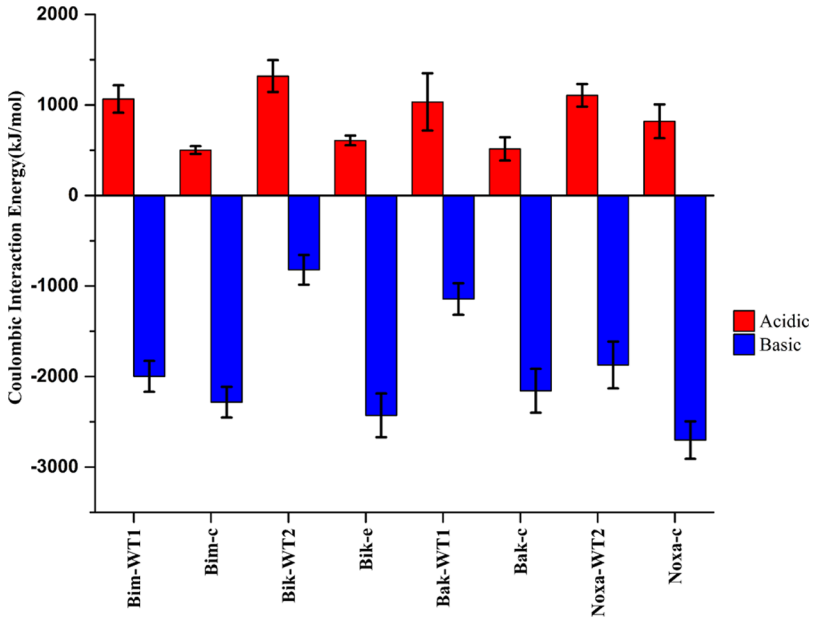

Figure 9. Average electrostatic interaction energies of BHRF1 in complex with BH3-like sequences Bim-c, Bik-e, Bak-c, and Noxa-c calculated from MD-simulated structures. For comparison purpose, average electrostatic interaction energies of BHRF1 in complex with the respective wild-type BH3 peptides are also shown. Electrostatic interactions calculated for acidic (red) and basic (blue) residues of the BH3 or BH3-like peptides are displayed separately.

https://doi.org/10.1021/acsomega.1c03385
ACS Omega 2021, 6, 26976−26989

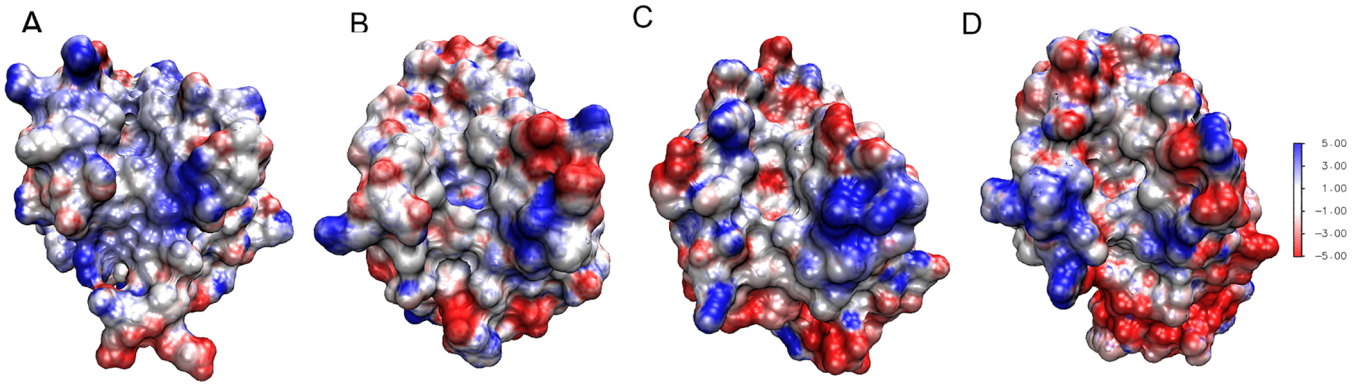

Figure 10. Electrostatic potential maps of (A) Mcl-1, (B) A179L, (C) BHRF1, and (D) Bcl-X_L calculated, respectively, using the experimentally determined structures with PDB IDs 2ROD, 5AU4, 2XPX, and 2BZW. The electrostatic potentials were deduced by solving the Poisson−Boltzmann equation utilizing Adaptive Poisson−Boltzmann Solver (APBS)[60] plugin of the VMD software package.[61] Red and blue colors in the diagrams correspond to negative and positive potentials, respectively.

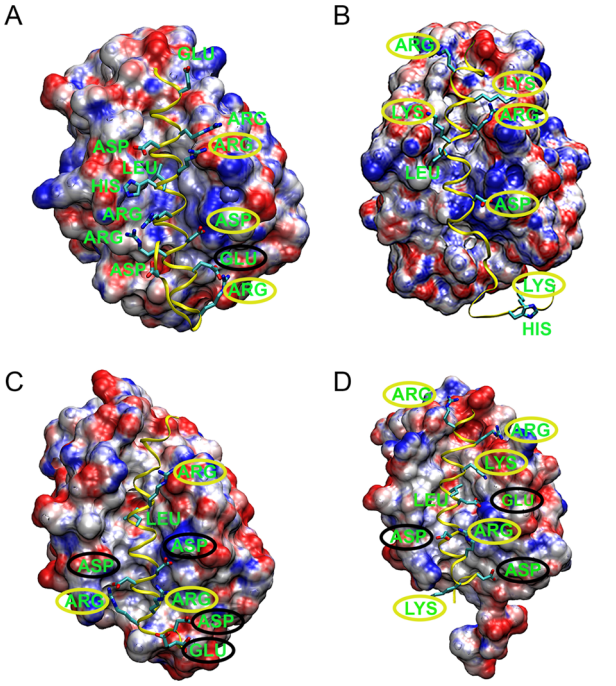

Figure 11. Electrostatic potential maps calculated for the MD-simulated structures of A179 when it was bound to the (A) wild-type Bid BH3 peptide and (B) Bid-based Bid-5 BH3-like peptide. Electrostatic potentials of MD-simulated BHRF1 structures when the protein was in complex with the (C) Bak wild-type BH3 peptide and (D) Bak-c, a BH3-like peptide derived from the wild-type Bak BH3 peptide. The MD-simulated structures were saved at the end of 500 ns production runs. For details of electrostatic calculations, see Figure 10. Charged residues that are involved in favorable and unfavorable interactions are circled in yellow and black colors, respectively.

electrostatic potential of all the four proteins reveals that Mcl-1 has mostly the basic patch around the BH3-binding pocket (Figure 10A). However, in A179L, additional regions of negative electrostatic potential are found (Figure 10B) and the acidic patch has further expanded in BHRF1 (Figure 10C). Bcl-X_L seems to have the most acidic patch in the region where the BH3 peptide binds (Figure 10D). This explains the preference of charged residues in BH3-like sequences that can bind to the vBcl-2 homologues A179L and BHRF1. While BH3-like sequences enriched in acidic residues bind favorably with Mcl-1,[52] both acidic and basic residues interact favorably with A179L. Both BHRF1 and Bcl-X_L prefer to bind BH3-like sequences which are rich in basic residues. We have also argued that the presence of charged residues in the hydrophilic face of the BH3 amphipathic helix can influence the binding of BH3 peptides as the electrostatic interactions are long range in nature. As a result, the so-called nonhotspot residues seem to play a significant role in the affinity of the BH3-mimetic peptides. Although the four conserved hydrophobic residues in the BH3 region can help in binding the hydrophobic groove of the prosurvival proteins, other residues from the peptide can exert significant influence while interacting with the residues of the protein. Our current study along with our earlier observation that the long-range electrostatic interactions can determine the affinity of BH3 peptides in binding to antiapoptotic Bcl-2 proteins[52] has to be incorporated while designing inhibitors to both mammalian and vBcl-2 homologues.

Critique of Methodology. Banjara et al. have recently reported the binding affinities of different proapoptotic BH3 peptides for A179L using isothermal titration calorimetry measurements.[29] It should be noted that the interaction energies calculated between the wild-type BH3 peptides and the protein reported in this study cannot be directly related to experimental binding affinities. Our comparison of interaction energies is "within" a specific wild-type BH3 peptide and the peptides derived from them. We are not comparing across the different BH3 peptides for two reasons. The four conserved hydrophobic residues recognize and interact with the hydrophobic groove of the protein, and they are not the same in all wild-type BH3 peptides, although the hydrophobic character is maintained. When we derived BH3-like peptides from wild-type proapoptotic BH3 peptides, we have retained the wild-type residues in these positions to make sure that the recognition process and interaction of BH3-like peptides are similar to that of wild-type peptides. This is also demonstrated experimentally by Keating and her colleagues.[64,65] When some of the positions occupied by conserved hydrophobic residues are substituted by Ala, there is a drastic change in the binding affinities for the antiapoptotic proteins Mcl-1 and Bcl-X_L. Similarly, when the highly conserved Leu was substituted by Tyr in Bim, the peptide no longer bound to Mcl-1. However, it was binding to Bcl-X_L and was selective for that protein. Hence, the differences observed in the four hydrophobic

https://doi.org/10.1021/acsomega.1c03385
ACS Omega 2021, 6, 26976−26989

positions in different wild-type proapoptotic BH3 peptides play a greater role in influencing binding and selectivity. Hence, we retained these four hydrophobic residues and another highly conserved Asp residue while substituting other positions randomly without any bias. This assured us that the binding mode of the wild-type BH3 peptide and its derivatives will be the same as that of the wild-type BH3 region, while the substitutions in other positions can indicate whether the interaction energies are further strengthened or weakened. Thus, we have consciously avoided comparing the interaction energies of different wild-type BH3 peptides, and our comparison is restricted to BH3-like peptides derived from the same wild-type BH3 peptide.

The second reason is that prediction of binding selectivity using computational methods is a complex and challenging problem. Calculating binding affinity requires a rigorous computational framework involving free-energy calculations and sophisticated treatment of force fields. Such methods have been applied to bromodomains, JNK1 kinase, p38, and the ovomucoid third domain.[66−68] These studies have used free-energy perturbation or thermodynamic integration methods. In this paper, our aim is not to reproduce the experimental binding affinities of wild-type BH3 peptides using computational methods. This computational approach is to identify BH3-like peptides derived from the wild-type proapoptotic BH3 region that are predicted to have enhanced binding affinity for the viral homologues. By retaining the conserved hydrophobic residues and the conserved Asp residue and by substituting positions that can be considered as nonhotspot residues, we make sure that the binding process is the same as the wild-type BH3 peptides and the substitutions in nonhotspot positions can give rise to additional favorable interactions. For this purpose, interaction energies of BH3-like peptides relative to their respective wild-type BH3 peptides are used. This approach has been validated experimentally in our earlier studies.[52]

CONCLUSIONS

Although the Bcl-2 homologues in viruses are distantly related to the mammalian antiapoptotic Bcl-2 proteins with strikingly similar three-dimensional fold, they have emerged as attractive drug targets that will have the potential to prevent viral infection. African swine flu virus causes one of the most dangerous and fatal infectious diseases in domestic pigs, and hence, molecules that can inhibit viral infection can help many economically affected countries. EBV has been implicated in human cancers including Hodgkin's and Burkitt's lymphoma. Structures of vBcl-2 homologues of both these viruses, A179L and BHRF1, adopt a typical Bcl-2 helical fold. With few studies available that focus on developing inhibitors to target A179L and BHRF1, the current study has used a computational approach to design peptides that can bind to the hydrophobic groove of these vBcl-2s. The designed peptide sequences selected from a library of BH3-like sequences have retained the original four conserved hydrophobic residues and a conserved Asp residue. The peptides have helical propensities significantly higher than the wild-type proapoptotic BH3 peptides. The unbiased selection of these peptides from the histogram of peptide/protein interaction energies revealed that the selected peptides are rich in basic residues. While A179L interacted favorably with both acidic and basic residues of the selected BH3-like peptides, the BHRF1 highly preferred peptides with basic residues and its interaction with acidic residues was clearly unfavorable. Analysis of electrostatic potential energy maps helped understand the differences between mammalian antiapoptotic Bcl-2 proteins and vBcl-2s. The Coulombic interactions between the BH3-like peptides and the proteins predominantly contribute to the protein/peptide interaction energy. This is true for both the mammalian prosurvival Bcl-2 proteins and vBcl-2s. This approach can be extended to other vBcl-2s, and the conclusions reached in this study can be incorporated in designing inhibitors that can specifically bind to A179L or BHRF1.

MATERIALS AND METHODS

Generation of BH3-like Sequences and Modeling the vBcl-2/BH3 Peptide Complex Structures. We have adopted the same approach which we used to design BH3-mimetic peptides for the mammalian antiapoptotic proteins Mcl-1 and Bcl-X_L in our earlier study.[52] Briefly, a library of BH3-like peptides was generated from the selected wild-type proapoptotic BH3 peptide. In this step, the conserved four hydrophobic residues and the Asp residue were retained in their original positions, and all other positions were substituted randomly without any bias. We considered the wild-type BH3 regions of eight proapoptotic proteins, namely, Puma, Noxa, Bmf, Bim, Bik, Bid, Bak, and Bad, and their BH3-domain sequences are shown in Figure 1. We employed the "Random Protein Regions" module of Sequence Manipulation suite web server (https://www.bioinformatics.org/sms2/random_protein_regions.html)[69] for this purpose. For each proapoptotic BH3 peptide, we generated 1000 randomized BH3-like sequences.

The randomly generated BH3-like sequences were used to model complex structures using the experimentally determined BHRF1 or A179L structures. For all wild-type proapoptotic BH3 peptides for which complex structures are yet to be determined with A179L and for all randomly generated BH3-like sequences, the experimentally determined A179L/Bid complex structure (PDB ID: 5UA4)[29] was used as the template structure. Structures of BHRF1 in complex with Bim (PDB ID: 2WH6) and Bak (PDB ID: 2XPX) are available in PDB.[20] However, examination of these structures reveals that there are missing regions in both the structures, and hence, we used both as template structures while modeling wild-type proapoptotic BH3 peptides or BH3-like sequences generated randomly. We used Modeller 9.14[70−72] to model the complex structures, and the protocol used to model the complex structures is the same as described previously.[52] Briefly, the experimentally determined structures of A179L and BHRF1 in complex with BH3 peptides were used to model the protein in complex with BH3/BH3-like peptides (see Figure 1 for details of template structures used). In all cases, the protein is the same (A179L or BHRF1) and only the peptides will differ. Since the critical step in Modeller is to correctly align the template-target sequences, this step boils down to correctly align the BH3 wild-type peptide in the template structure and the BH3-like sequences in the target. It should be noted that while generating the BH3-like sequences from the wild-type proapoptotic BH3 regions, the four conserved hydrophobic residues and the conserved Asp residue were not changed. Hence, aligning the target-template sequences is straightforward. All other details are exactly the same as that given in our previous publication.[52] For each BH3-like sequence, we used this modeling procedure to generate five best models which were further energy-minimized in a water box using the

https://doi.org/10.1021/acsomega.1c03385
ACS Omega 2021, 6, 26976−26989

GROMACS 4.5.5 software suite.[73] Each modeled protein/peptide complex structure was solvated using the SPC/E water model,[74] and the OPLS/AA force field[75] was used in the minimization protocol. Short- and long-range interactions were evaluated for the nonbonded pairs that were within a cutoff of 10 Å and within 10−25 Å, respectively. Among the five selected models, the model with minimum potential energy was selected to calculate the interaction energy between the peptide and protein as given in the following equation.

$$E_{int} = E_{AB} - (E_A + E_B) \quad (1)$$

where E_{AB}, E_A, and E_B represent the potential energies of the complex structure, the protein A179L/BHRF1, and the wild-type BH3/BH3-like peptide, respectively. Interaction energies were calculated between the wild-type BH3 or the BH3-like sequences and the protein. In total, we modeled 16,000 structures (1000 BH3-like sequences generated each for the eight wild-type BH3 sequences, and the two sets of 8000 sequences thus generated were used to build A179L and BHRF1 complex structures). Histograms of interaction energies for A179L and BHRF1 complex structures were plotted for BH3-like sequences derived based on each of the eight wild-type BH3 sequences. We also determined the helicity of each BH3-like sequence using Agadir web server at 278 K, pH 7, and 0.1 M ionic strength.[56−58] The amphipathic nature of each BH3-like sequence was determined by quantifying the mean helical hydrophobic moment using the HeliQuest web server.[59]

MD Simulation of Selected Complex Structures. We performed MD simulations of selected models of A179L and BHRF1 structures in complex with BH3-like sequences. Simulations were carried out following the same protocol used in our earlier studies.[52] In each case, the complex structure was first solvated using the SPC/E water model[74] in a cubic box, and the minimum distance between the complex and the wall of the box was at least 13 Å. The systems were neutralized by adding the required number of counterions and then energy-minimized. The OPLS all-atom force field[75] was used, and the simulations were performed using GROMACS 5.1.4.[73,76] The equilibration step consisted of 1 ns simulation in the *NVT* ensemble with positional restraints (force constant 2000 kJ/mol nm) on all heavy atoms. This was followed by 1.8 ns simulation in the *NPT* ensemble in which the positional restraints were gradually removed on all atoms except the backbone atoms. Restraints on backbone atoms were gradually removed over a period of another 2 ns simulation in the *NPT* ensemble to ensure that the modeled BH3 peptide helix is properly equilibrated. After the equilibration, each system was simulated for a period of 500 ns. The system was maintained at the reference temperature 300 K. All other details were same as given in Reddy et al.[52] Summary of all the systems simulated is provided in Table S1. A total of 7 μs simulation was carried out for all the systems. The coordinates were saved every 10 ps, and 50,000 MD-simulated structures were used for further analysis for each system. Helix stability of BH3-like peptides, interaction energies between the peptide and protein, and contribution of acidic and basic residues for the protein/peptide interaction energies were analyzed in MD simulations. Interaction energy between the protein and the peptide for each MD-simulated structure was calculated using eq 1. A twin-range cutoff of 10 to 25 Å was used for the purpose of calculating the interaction energy between the peptide and protein for all the MD-simulated structures.

DATA AND SOFTWARE AVAILABILITY

As mentioned in the Materials and Methods section, randomized BH3 sequences were generated using Sequence Manipulation suite software available at https://www.bioinformatics.org/sms2/. Homology models were generated using Modeller v 9.14 (https://salilab.org/modeller/). Agadir was used to predict the helical content of BH3-like peptides (https://agadir.crg.es/). Mean helical hydrophobic moments of the BH3-like sequences were calculated using HeliQuest (https://heliquest.ipmc.cnrs.fr/). Minimum energies of all A179L/BHRF1−BH3 peptide complex structures were calculated using the program GROMACS 4.5.5 (www.gromacs.org). MD simulations of selected protein/peptide complex structures were performed using the GROMACS 5.1.4 version. All the data are presented in the manuscript and Supporting Information.

ASSOCIATED CONTENT

Supporting Information

The Supporting Information is available free of charge at https://pubs.acs.org/doi/10.1021/acsomega.1c03385.

Figures of helical propensities and mean helical hydrophobic moments of wild-type BH3 and selected BH3-like sequences, van der Waals component of interaction energies between BH3 peptides and A179L/BHRF1 proteins, initial and MD-simulated structures saved at the end of the production runs for A179L/BHRF1 in complex with BH3 peptides, and tables summarizing the MD simulations of A179L/BHRF1−BH3peptide complex structures and the interaction energies between the peptide charges residues and proteins (PDF)

AUTHOR INFORMATION

Corresponding Author

Ramasubbu Sankararamakrishnan − *Department of Biological Sciences and Bioengineering and Mehta Family Center for Engineering in Medicine, Indian Institute of Technology Kanpur, Kanpur 208016, India;* orcid.org/0000-0002-8527-5614; Phone: +91 512 259 4014; Email: rsankar@iitk.ac.in; Fax: +91 512 259 4010

Author

Chinthakunta Narendra Reddy − *Department of Biological Sciences and Bioengineering, Indian Institute of Technology Kanpur, Kanpur 208016, India*

Complete contact information is available at: https://pubs.acs.org/10.1021/acsomega.1c03385

Notes

The authors declare no competing financial interest.

ACKNOWLEDGMENTS

We gratefully acknowledge the High Performance Computing Facility at IIT-Kanpur. R.S. is Pradeep Sindhu Chair Professor. C.N.R. thanks BINC Fellowship from the Department of Biotechnology (DBT), Government of India. R.S. thanks IIT-Kanpur for the financial support.

REFERENCES

(1) Elmore, S. Apoptosis: A review of programmed cell death. *Toxicol. Pathol.* **2007**, 35, 495−516.

(2) Youle, R. J.; Strasser, A. The BCL-2 protein family: opposing activities that mediate cell death. *Nat. Rev. Mol. Cell Biol.* **2008**, *9*, 47−59.
(3) Adams, J. M.; Cory, S. Life-or-death decisions by the Bcl-2 protein family. *Trends Biochem. Sci.* **2001**, *26*, 61−66.
(4) Chao, D. T.; Korsmeyer, S. J. Bcl-2 family: Regulators of cell death. *Annu. Rev. Immunol.* **1998**, *16*, 395−419.
(5) Banjara, S.; Suraweera, C. D.; Hinds, M. G.; Kvansakul, M. The Bcl-2 family: Ancient origins, conserved structures, and divergent mechanisms. *Biomolecules* **2020**, *10*, 128.
(6) Kuwana, T.; Bouchier-Hayes, L.; Chipuk, J. E.; Bonzon, C.; Sullivan, B. A.; Green, D. R.; Newmeyer, D. D. BH3 domains of BH3-Only proteins differentially regulate Bax-mediated mitochondrial membrane permeabilization both directly and indirectly. *Mol. Cell* **2005**, *17*, 525−535.
(7) Huang, D. C. S.; Strasser, A. BH3-only proteins-Essential initiators of apoptotic cell death. *Cell* **2000**, *103*, 839−842.
(8) Scorrano, L.; Korsmeyer, S. J. Mechanisms of cytochrome c release by pro-apoptotic BCL-2 family members. *Biochem. Biophys. Res. Commun.* **2003**, *304*, 437−444.
(9) Dewson, G.; Kluck, R. M. Mechanisms by which Bak and Bax permeabilise mitichondria during apoptosis. *J. Cell Sci.* **2009**, *122*, 2801−2808.
(10) Galluzzi, L.; Brenner, C.; Morselli, E.; Touat, Z.; Kroemer, G. Viral control of mitochondrial apoptosis. *PLoS Pathog.* **2008**, *4*, No. e1000018.
(11) Cuconati, A.; White, E. Viral homologs of BCL-2: role of apoptosis in the regulation of virus infection. *Genes Dev.* **2002**, *16*, 2465−2478.
(12) Thomson, I.; Pershin, V.; Mostaghimi, J.; Chandra, S. Viruses and apoptosis. *Int. J. Exp. Pathol.* **2001**, *21*, 65−82.
(13) Kvansakul, M.; Hinds, M. G. Structural biology of the Bcl-2 family and its mimicry by viral proteins. *Cell Death Dis.* **2013**, *4*, No. e909.
(14) Kvansakul, M.; Caria, S.; Hinds, M. The Bcl-2 family in host-virus interactions. *Viruses* **2017**, *9*, 290.
(15) Petros, A. M.; Olejniczak, E. T.; Fesik, S. W. Structural biology of the Bcl-2 family of proteins. *Biochim. Biophys. Acta* **2004**, *1644*, 83−94.
(16) Lama, D.; Sankararamakrishnan, R. Identification of core structural residues in the sequentially diverse and structurally homologous Bcl-2 family of proteins. *Biochemistry* **2010**, *49*, 2574−2584.
(17) Kvansakul, M.; Yang, H.; Fairlie, W. D.; Czabotar, P. E.; Fischer, S. F.; Perugini, M. A.; Huang, D. C. S.; Colman, P. M. Vaccinia virus anti-apoptotic F1L is a novel Bcl-2-like domain-swapped dimer that binds a highly selective subset of BH3-containing death ligands. *Cell Death Differ.* **2008**, *15*, 1564−1571.
(18) Cooray, S.; Bahar, M. W.; Abrescia, N. G. A.; McVey, C. E.; Bartlett, N. W.; Chen, R. A.-J.; Stuart, D. I.; Grimes, J. M.; Smith, G. L. Functional and structural studies of the vaccinia virus virulence factor N1 reveal a Bcl-2-like anti-apoptotic protein. *J. Gen. Virol.* **2007**, *88*, 1656−1666.
(19) Douglas, A. E.; Corbett, K. D.; Berger, J. M.; McFadden, G.; Handel, T. M. Structure of M11L: A myxoma virus structural homolog of the apoptosis inhibitor, Bcl-2. *Protein Sci.* **2007**, *16*, 695−703.
(20) Kvansakul, M.; Wei, A. H.; Fletcher, J. I.; Willis, S. N.; Chen, L.; Roberts, A. W.; Huang, D. C. S.; Colman, P. M. Structural basis for apoptosis inhibition by Epstein-Barr virus BHRF1. *PLoS Pathog.* **2010**, *6*, No. e1001236.
(21) Huang, Q.; Petros, A. M.; Virgin, H. W.; Fesik, S. W.; Olejniczak, E. T. Solution structure of a Bcl-2 homolog from Kaposi sarcoma virus. *Proc. Natl. Acad. Sci. U.S.A.* **2002**, *99*, 3428−3433.
(22) Marshall, B.; Puthalakath, H.; Caria, S.; Chugh, S.; Doerflinger, M.; Colman, P. M.; Kvansakul, M. Variola virus F1L is a Bcl-2-like protein that unlike its vaccinia virus counterpart inhibits apoptosis independent of Bim. *Cell Death Dis.* **2015**, *6*, No. e1680.
(23) Loh, J.; Huang, Q.; Petros, A. M.; Nettesheim, D.; van Dyk, L. F.; Labrada, L.; Speck, S. H.; Levine, B.; Olejniczak, E. T.; Virgin, H. W., IV A surface groove essential for viral Bcl-2 function during chronic infection in vivo. *PLoS Pathog.* **2005**, *1*, No. e10.
(24) Suraweera, C. D.; Hinds, M. G.; Kvansakul, M. Crystal structures of ORFV125 provide insight into orf virus-mediated inhibition of apoptosis. *Biochem. J.* **2020**, *477*, 4527−4541.
(25) Banjara, S.; Mao, J.; Ryan, T. M.; Caria, S.; Kvansakul, M. Grouper iridovirus GIV66 is a Bcl-2 protein that inhibits apoptosis by exclusively sequestering Bim. *J. Biol. Chem.* **2018**, *293*, 5464−5477.
(26) Anasir, M.; Baxter, A.; Poon, I.; Hulett, M.; Kvansakul, M. Structural and functional insight into Canarypox virus CNP058 mediated regulation of apoptosis. *Viruses* **2017**, *9*, 305.
(27) Anasir, M. I.; Caria, S.; Skinner, M. A.; Kvansakul, M. Structural basis of apoptosis inhibition by the fowlpox virus protein FPV039. *J. Biol. Chem.* **2017**, *292*, 9010−9021.
(28) Suraweera, C. D.; Anasir, M. I.; Chugh, S.; Javorsky, A.; Impey, R. E.; Hasan Zadeh, M.; Soares da Costa, T. P.; Hinds, M. G.; Kvansakul, M. Structural insight into tanapoxvirus-mediated inhibition of apoptosis. *FEBS J.* **2020**, *287*, 3733−3750.
(29) Banjara, S.; Caria, S.; Dixon, L. K.; Hinds, M. G.; Kvansakul, M. Structural insight into African swine fever virus A179L-mediated inhibition of apoptosis. *J. Virol.* **2017**, *91*, e02228−16.
(30) Giddens, W. E.; Swango, L. J.; Henderson, J. D.; Lewis, R. A.; Farner, D. S.; Carlos, A.; Dolowy, W. C. Canary pox in sparrows and canaries (Fringillidae) and in weavers (Ploceidae); Pathology and Host Specificity of the Virus. *Vet. Pathol.* **1971**, *8*, 260−280.
(31) Kerr, P. J.; Best, S. M. Myxoma virus in rabbits. *Rev. Sci. Tech.* **1998**, *17*, 256−268.
(32) Young, L. S.; Rickinson, A. B. Epstein-Barr virus: 40 years on. *Nat. Rev. Cancer* **2004**, *4*, 757−768.
(33) Parravicini, C.; Chandran, B.; Corbellino, M.; Berti, E.; Paulli, M.; Moore, P. S.; Chang, Y. Differential viral protein expression in Kaposi's sarcoma-associated herpesvirus-infected diseases: Kaposi's sarcoma, primary effusion lymphoma, and multicentric Castleman's disease. *Am. J. Pathol.* **2000**, *156*, 743−749.
(34) Spyrou, V.; Valiakos, G. Orf virus infection in sheep or goats. *Vet. Microbiol.* **2015**, *181*, 178−182.
(35) Chua, F. H. C.; Ng, M. L.; Ng, K. L.; Loo, J. J.; Wee, J. Y. Investigation of outbreaks of a novel disease, 'Sleepy Grouper Disease', affecting the brown-spotted grouper, *Epinephelus tauvina* Forskal. *J. Fish Dis.* **1994**, *17*, 417−427.
(36) Tripathy, D. N.; Hanson, L. E. Pathogenesis of fowlpox in laying hens. *Avian Dis.* **1978**, *22*, 259−265.
(37) Revilla, Y.; Pérez-Núñez, D.; Richt, J. A. African swine fever virus biology and vaccine approaches. *Adv. Virus Res.* **2018**, *100*, 41−74.
(38) Sattler, M.; Liang, H.; Nettesheim, D.; Meadows, R. P.; Harlan, J. E.; Eberstadt, M.; Yoon, H. S.; Shuker, S. B.; Chang, B. S.; Minn, A. J.; Thompson, C. B.; Fesik, S. W. Structure of Bcl-x_L-Bak peptide complex: Recognition between regulators of apoptosis. *Science* **1997**, *275*, 983−986.
(39) Chittenden, T.; Flemington, C.; Houghton, A. B.; Ebb, R. G.; Gallo, G. J.; Elangovan, B.; Chinnadurai, G.; Lutz, R. J. A conserved domain in Bak, distinct from BH1 and BH2, mediates cell death and protein binding functions. *EMBO J.* **1995**, *14*, 5589−5596.
(40) Chen, L.; Willis, S. N.; Wei, A.; Smith, B. J.; Fletcher, J. I.; Hinds, M. G.; Colman, P. M.; Day, C. L.; Adams, J. M.; Huang, D. C. S. Differential targeting of prosurvival Bcl-2 proteins by their BH3-only ligands allows complementary apoptotic function. *Mol. Cell* **2005**, *17*, 393−403.
(41) Kong, W.; Zhou, M.; Li, Q.; Fan, W.; Lin, H.; Wang, R. Experimental characterization of the binding affinities between proapoptotic BH3 peptides and antiapoptotic Bcl-2 proteins. *ChemMedChem* **2018**, *13*, 1763−1770.
(42) Kvansakul, M.; van Delft, M. F.; Lee, E. F.; Gulbis, J. M.; Fairlie, W. D.; Huang, D. C. S.; Colman, P. M. A structural viral mimic of prosurvival Bcl-2: A pivotal role for sequestering proapoptotic Bax and Bak. *Mol. Cell* **2007**, *25*, 933−942.

https://doi.org/10.1021/acsomega.1c03385
ACS Omega 2021, 6, 26976−26989

(43) Okamoto, T.; Campbell, S.; Mehta, N.; Thibault, J.; Colman, P. M.; Barry, M.; Huang, D. C. S.; Kvansakul, M. Sheeppox virus SPPV14 encodes a Bcl-2-like cell death inhibitor that counters a distinct set of mammalian proapoptotic proteins. *J. Virol.* **2012**, *86*, 11501−11511.
(44) Flanagan, A. M.; Letai, A. BH3 domains define selective inhibitory interactions with BHRF-1 and KSHV BCL-2. *Cell Death Differ.* **2008**, *15*, 580−588.
(45) Aoyagi, M.; Zhai, D.; Jin, C.; Aleshin, A. E.; Stec, B.; Reed, J. C.; Liddington, R. C. Vaccinia virus N1L protein resembles a B cell lymphoma-2 (Bcl-2) family protein. *Protein Sci.* **2007**, *16*, 118−124.
(46) Ashkenazi, A.; Fairbrother, W. J.; Leverson, J. D.; Souers, A. J. From basic apoptosis discoveries to advanced selective BCL-2 family inhibitors. *Nat. Rev. Drug Discovery* **2017**, *16*, 273−284.
(47) Vogler, M.; Dinsdale, D.; Dyer, M. J. S.; Cohen, G. M. Bcl-2 inhibitors: small molecules with a big impact on cancer therapy. *Cell Death Differ.* **2009**, *16*, 360−367.
(48) Robert, A.; Pujals, A.; Favre, L.; Debernardi, J.; Wiels, J. The BCL-2 family protein inhibitor ABT-737 as an additional tool for the treatment of EBV-associated post-transplant lymphoproliferative disorders. *Mol. Oncol.* **2020**, *14*, 2520−2532.
(49) Burrer, C. M.; Foight, G. W.; Keating, A. E.; Chan, G. C. Selective peptide inhibitors of antiapoptotic cellular and viral Bcl-2 proteins lead to cytochrome c release during latent Kaposi's sarcoma-associated herpesvirus infection. *Virus Res.* **2016**, *211*, 86−88.
(50) Caria, S.; Chugh, S.; Nhu, D.; Lessene, G.; Kvansakul, M. Crystallization and preliminary X-ray characterization of Epstein-Barr virus BHRF1 in complex with a benzoylurea peptidomimetic. *Acta Crystallogr., Sect. F: Struct. Biol. Cryst. Commun.* **2012**, *68*, 1521−1524.
(51) Procko, E.; Berguig, G. Y.; Shen, B. W.; Song, Y.; Frayo, S.; Convertine, A. J.; Margineantu, D.; Booth, G.; Correia, B. E.; Cheng, Y.; Schief, W. R.; Hockenbery, D. M.; Press, O. W.; Stoddard, B. L.; Stayton, P. S.; Baker, D. A computationally designed inhibitor of an Epstein-Barr viral Bcl-2 protein induces apoptosis in infected cells. *Cell* **2014**, *157*, 1644−1656.
(52) Reddy, C. N.; Manzar, N.; Ateeq, B.; Sankararamakrishnan, R. Computational design of BH3-mimetic peptide inhibitors that can bind specifically to Mcl-1 or Bcl-XL: Role of non-hot spot residues. *Biochemistry* **2020**, *59*, 4379−4394.
(53) Lama, D.; Sankararamakrishnan, R. Molecular dynamics simulations of pro-apoptotic BH3 peptide helices in aqueous medium: relationship between helix stability and their binding affinities to anti-apoptotic protein Bcl-XL. *J. Comput.-Aided Mol. Des.* **2011**, *25*, 413−426.
(54) Modi, V.; Lama, D.; Sankararamakrishnan, R. Relationship between helix stability and binding affinities: molecular dynamics simulations of Bfl-1/A1-binding pro-apoptotic BH3 helices in explicit solvent. *J. Biomol. Struct. Dyn.* **2013**, *31*, 65−77.
(55) Petros, A. M.; Nettesheim, D. G.; Wang, Y.; Olejniczak, E. T.; Meadows, R. P.; Mack, J.; Swift, K.; Matayoshi, E. D.; Zhang, H.; Thompson, C. B.; Fesik, S. W. Rationale for Bcl-XL/Bad peptide complex formation from structure, mutagenesis, and biophysical studies. *Protein Sci.* **2000**, *9*, 2528−2534.
(56) Muñoz, V.; Serrano, L. Elucidating the folding problem of helical peptides using empirical parameters. *Nat. Struct. Mol. Biol.* **1994**, *1*, 399−409.
(57) Muñoz, V.; Serrano, L. Elucidating the folding problem of helical peptides using empirical parameters. II. Helix macrodipole effects and rational modification of the helical content of natural peptides. *J. Mol. Biol.* **1995**, *245*, 275−296.
(58) Muñoz, V.; Serrano, L. Elucidating the folding problem of helical peptides using empirical parameters. III. Temperature and pH dependence. *J. Mol. Biol.* **1995**, *245*, 297−308.
(59) Gautier, R.; Douguet, D.; Antonny, B.; Drin, G. HELIQUEST: a web server to screen sequences with specific α-helical properties. *Bioinformatics* **2008**, *24*, 2101−2102.
(60) Baker, N. A.; Sept, D.; Joseph, S.; Holst, M. J.; McCammon, J. A. Electrostatics of nanosystems: Application to microtubules and the ribosome. *Proc. Natl. Acad. Sci. U.S.A.* **2001**, *98*, 10037−10041.
(61) Humphrey, W.; Dalke, A.; Schulten, K. VMD: Visual molecular dynamics. *J. Mol. Graphics Modell.* **1996**, *14*, 33−38.
(62) Day, C. L.; Smits, C.; Fan, F. C.; Lee, E. F.; Fairlie, W. D.; Hinds, M. G. Structure of the BH3 domains from the p53-inducible BH3-only proteins Noxa and Puma in complex with Mcl-1. *J. Mol. Biol.* **2008**, *380*, 958−971.
(63) Ivanov, S. M.; Huber, R. G.; Warwicker, J.; Bond, P. J. Energetics and dynamics across the Bcl-2-regulated apoptotic pathway reveal distinct evolutionary determinants of specificity and affinity. *Structure* **2016**, *24*, 2024−2033.
(64) Dutta, S.; Gullá, S.; Chen, T. S.; Fire, E.; Grant, R. A.; Keating, A. E. Determinants of BH3 binding specificity for Mcl-1 versus Bcl-X_L. *J. Mol. Biol.* **2010**, *398*, 747−762.
(65) Fire, E.; Gullá, S. V.; Grant, R. A.; Keating, A. E. Mcl-1-Bim complexes accommodate surprising point mutations via minor structural changes. *Protein Sci.* **2010**, *19*, 507−519.
(66) Wang, L.; Wu, Y.; Deng, Y.; Kim, B.; Pierce, L.; Krilov, G.; Lupyan, D.; Robinson, S.; Dahlgren, M. K.; Greenwood, J.; Romero, D. L.; Masse, C.; Knight, J. L.; Steinbrecher, T.; Beuming, T.; Damm, W.; Harder, E.; Sherman, W.; Brewer, M.; Wester, R.; Murcko, M.; Frye, L.; Farid, R.; Lin, T.; Mobley, D. L.; Jorgensen, W. L.; Berne, B. J.; Friesner, R. A.; Abel, R. Accurate and reliable prediction of relative ligand binding potency in prospective drug discovery by way of a modern free-energy calculation protocol and force field. *J. Am. Chem. Soc.* **2015**, *137*, 2695−2703.
(67) Aldeghi, M.; Heifetz, A.; Bodkin, M. J.; Knapp, S.; Biggin, P. C. Predictions of ligand selectivity from absolute binding free energy calculations. *J. Am. Chem. Soc.* **2017**, *139*, 946−957.
(68) Zou, J.; Simmerling, C.; Raleigh, D. P. Dissecting the energetics of intrinsically disordered proteins via a hybrid experimental and computational approach. *J. Phys. Chem. B* **2019**, *123*, 10394−10402.
(69) Stothard, P. The sequence manipulation suite: Javascript programs for analyzing and formatting protein and DNA sequences. *Biotechniques* **2000**, *28*, 1102−1104.
(70) Webb, B.; Sali, A. Comparative protein structure modeling using MODELLER. *Curr. Protoc. Bioinf.* **2014**, *47*, 5.6.1−5.6.32.
(71) Eswar, N.; Eramian, D.; Webb, B.; Shen, M.-Y.; Sali, A. Protein structure modeling with MODELLER. *Methods Mol. Biol.* **2008**, *426*, 145−159.
(72) Sali, A.; Blundell, T. L. Comparative protein modelling by satisfaction of spatial restraints. *J. Mol. Biol.* **1993**, *234*, 779−815.
(73) Pronk, S.; Páll, S.; Schulz, R.; Larsson, P.; Bjelkmar, P.; Apostolov, R.; Shirts, M. R.; Smith, J. C.; Kasson, P. M.; van der Spoel, D.; Hess, B.; Lindahl, E. GROMACS 4.5: a high-throughput and highly parallel open source molecular simulation toolkit. *Bioinformatics* **2013**, *29*, 845−854.
(74) Berendsen, H. J. C.; Grigera, J. R.; Straatsma, T. P. The missing term in effective pair potentials. *J. Phys. Chem.* **1987**, *91*, 6269−6271.
(75) Jorgensen, W. L.; Maxwell, D. S.; Tirado-Rives, J. Development and testing of the OPLS all-atom force field on conformational energetics and properties of organic liquids. *J. Am. Chem. Soc.* **1996**, *118*, 11225−11236.
(76) Abraham, M. J.; Murtola, T.; Schulz, R.; Pall, S.; Smith, J. C.; Hess, B.; Lindahl, E. GROMACS: High performance molecular simulations through multi-level parallelism from laptops to supercomputers. *SoftwareX* **2015**, *1-2*, 19−25.

NOTE ADDED IN PROOF

Reference 76 was added to the Materials and Methods Section during production.

https://doi.org/10.1021/acsomega.1c03385
ACS Omega 2021, 6, 26976−26989